Journal of Hazardous Materials 416 (2021) 125717

Contents lists available at ScienceDirect

Journal of Hazardous Materials

journal homepage: www.elsevier.com/locate/jhazmat

Anaerobic mixed consortium (AMC) mediated enhanced biosynthesis of silver nano particles (AgNPs) and its application for the removal of phenol

A. Muthu Kumara Pandian [a,*], M. Rajasimman [b], N. Rajamohan [c], Sunita Varjani [d], C. Karthikeyan [b]

[a] Department of Biotechnology, Vivekanandha College of Engineering for Women, Namakkal, Tiruchengode 637205, India
[b] Environmental Engineering Laboratory, Department of Chemical Engineering, Annamalai University, Annamalai Nagar 608002, Tamilnadu, India
[c] Department of Chemical Engineering, Sohar University, Sohar 311, Oman
[d] Gujarat Pollution Control Board, Gandhi Nagar 382010, Gujarat, India

ARTICLE INFO

Editor: Dr. Rinklebe Jörg

Keywords:
Nanoparticle
Anaerobic mixed consortium
Phenol
Silver
RSM
Optimization

ABSTRACT

In this research, silver nano particle (AgNP), was synthesized through a novel anaerobic mixed consortium mediation method and applied for the removal of phenol. The best operating conditions for the fabrication of silver nanoparticles were identified through response surface methodology (RSM) and the maximum yield was found to be 2.65 g/100 ml of anaerobic mixed consortium at optimal conditions of pH-8.6, temperature-90 °C, silver nitrate concentration-3 mg/ml and inoculum volume-3 ml. The synthesized nano particle exhibited a maximum phenol removal of 87.65% was achieved at pH:5.8. The synthesized silver nanoparticles were characterized by superior surface area (19.26 m^2/g) and the stability was confirmed by thermo gravimetric analysis (upto 500 °C). The surface morphology was well explained using High Resolution Transmission Emission Microscopy (HR-TEM) and Scanning Electron Microscope with EDS (SEM-EDS) techniques. X-ray Diffraction (XRD) analysis confirmed the changes in crystalline structure due to the adsorption of phenol. Kinetic experiments fitted well with the intra-particle diffusion model. The nature of adsorption of phenol was confirmed as monolayer by the goodness of fit with Langmuir isotherm ($R^2 > 0.9969$).

1. Introduction

Nanotechnology is the latest and emerging field of research, which is consistently growing, building an impact in various aspects of human life (Mittal et al., 2014). Apart from the utilization of the specific potential that materials possess in nano dimensions (1–1000 nm), they also exhibit explicit transformed physical, chemical and biological properties in comparison to their macro counterparts (Rafique et al., 2017; Muthu Kumara Pandian et al., 2016). The reactivity of surface and more surface area which is a result of chemical reduction properties can be exploited as an alternate tool for environmental remediation (Rastogi and Arunachalam, 2013). Although technological advancements assists the production of nanoparticles with advanced physical and chemical approaches, the risk of generating enormous contaminants to environment with hazardous by products is higher.

Biological approach, an eco-friendly method, assisted by microorganisms presents a potential alternate technique which have significant advantages. A unique suggestion for the formulation of nanomaterials is the use of conventional fabrication process and a biological entity (Bansal et al., 2011; Mukherjee et al., 2001). In the case of microbial assisted production of nanoparticles, the microorganisms utilize the target ions from their environment. It employs the enzymes obtained through numerous cellular processes and converts the metal ions as the elemental metal. Microorganisms produce nanoparticles from inorganic materials through both intracellular as well as extracellular processes. As distinguished secretor of proteins, microorganisms hold the potential to deliver a higher yield of nanoparticles. Although nanoparticles are produced by microbes both by intracellular and extracellular processes, it is easier and convenient when they are synthesized extracellular. With their excessive secretary factor, they stabilize the nanoparticle through reduction and capping process. The quick and nonhazardous process of hydrolyzing the metal ions is enabled by the proteins present in the microbes. Colloidal structures are obtained as a result of biosynthesis of nanoparticles, involving reduction or oxidation of substrates. The formation of nanoparticles by the reduction of metal compounds is established by the enzymes present in the microorganisms possessing the

* Corresponding author.
E-mail address: dr.mkpandian@gmail.com (A. Muthu Kumara Pandian).

https://doi.org/10.1016/j.jhazmat.2021.125717
Received 19 December 2020; Received in revised form 6 March 2021; Accepted 19 March 2021
Available online 23 March 2021
0304-3894/© 2021 Elsevier B.V. All rights reserved.

capacity to reduce or act as antioxidants. Using nanoparticles produced through microbial approaches, eliminates various health associated risks, when the direct use of microbes in various related work is practiced.

Silver nanoparticles (AgNPs) are identified as potential nanomaterials suitable for applications in environmental pollution control are mostly related to their extremely active and high surface area per unit volume, specificity to attract pollutants by surface active functional groups and favorable surface plasmon resonance. Even though, synthesis of silver Nano particles was practiced using different approaches, namely, physical, chemical and biological approaches, the suitability of biological approach has gained momentum due to their eco-friendliness and cost effectiveness (Yasmin et al.,2020; Islam et al., 2021). Many studies on use of plant extracts have reported successful synthesis of silver nano particles. In spite of many research studies, there are no extensive studies in the application of microbial sources, especially anaerobic microbial consortia (AMC), for the synthesis of silver nano particles.

Rapid accumulation of recalcitrant chemicals in biosphere severely endangers environment and human health (Pishgar et al., 2012). Among these chemicals, phenolic compounds are identified as potentially carcinogenic and toxic substances. Apart from their lethal potential, phenol derivatives transmit an oxygen demand; impart taste and odor into the water even at a minimal concentration. Due to the continuous release of phenol and its derivatives from pharmaceutical, petroleum, coal transformation and phenol synthesizing industries, domestic water bodies are severely affected (Ihsan, 2013). As per the guideline of Environmental Protection Agency, a limit of 0.1 mg/L of phenol in waste water and 0.002 mg/L of phenol in drinking water is permissible. Hence there is a need to control and remediate phenol and its derivatives from the water ecosystem so as to reduce its hazardous impact. In recent years, adsorptive removal of phenol is investigated by various sorbents (Hamdaoui et al., 2018; Mohammed et al. 2018; Mingliang et al. 2019; Tabana et al. 2020; Lawal et al. 2020; Dehmani et al. 2020). Application of nanoparticles for the removal of phenol is a potential alternative and not explored in detail. In this research, synthesis of AgNPs was investigated using a novel anaerobic microbial consortia and the optimal conditions for maximum nano particle synthesis were identified using statistical methods. Detailed characterization of the nanoparticles synthesized were carried out to identify the surface properties, phase structure and thermal stability. The application of the silver nanoparticles synthesized using the anaerobic microbes was verified to remove phenol at different operating conditions. The mechanism of phenol removal was examined suing isotherm modeling and the reusability of the nanoparticles was verified through desorption studies.

2. Materials and methods

2.1. Materials

Silver nitrate, $AgNO_3$ (Himedia) and phenol (Merck Ltd.) were purchased. The deionized water was used to prepare the $AgNO_3$ solution and the prepared solution was stored in refrigerator in dark colored bottles in order to avoid photosensitive reaction of $AgNO_3$. Anaerobic mixed consortium was used to produce AgNPs. The anaerobic mixed consortium is obtained from the cow dung through serial dilution technique, followed by the plating and maintenance of the culture. The culture is maintained under anaerobic condition till the formation of the nanoparticles is confirmed.

2.2. Experimentation using RSM

The linear and interactive effects of variables on AgNP synthesis and phenol removal were studied using Box Behnken design (BBD). Design expert (7.1.5) was utilized to analyze phenol adsorption data. A second order model fitted to the experimental data was given by Eq. (1):

Table 1
Independent variable range and levels for Ag-NP production.

Factors	Range		
	-1	0	1
Temperature (°C)	30	60	90
pH	6	8	10
Concentration of $AgNO_3$ (mg/ml)	0.6	2	3.4
Inoculum Concentration (mg/ml)	1	2	3

Table 2
Independent variable range and levels for removal of phenol.

Factors	Range		
	-1	**0**	**1**
pH	5	7	9
Temperature(°C)	30	45	60
AgNP Dose (g)	0.1	0.5	0.9

$$Y = \beta_0 \quad + \sum_{i=1}^{k} \beta_i X_i + \sum_{i=1}^{k} \beta_{ii} X_i^2 + \sum i = 1_{k-1}^{\sum_{j=i+1}^{k} \beta_{ij}} X_{ij} \qquad (1)$$

where Y is the predicted response, β_i, β_{ii}, and β_{ij} are coefficients estimated from regression and represent the linear, quadratic and interaction effect respectively. β_0 is the intercept term. and X_i, X_j…. X_k represent the input variables in coded form.

2.3. Enhanced eco-friendly production of AgNP using BBD

To enhance the AgNP production by eco-friendly method, the parameters, namely temperature, pH, concentration of inoculum and concentration of $AgNO_3$ were optimized. The low and high levels of parameters were tabulated in Table 1.

2.4. AgNP Characterization

The AgNP formation is confirmed by monitoring the color transfer from pale white to dark brown. The AgNPs were then scanned in the spectral range of 200–800 nm for further confirmation. The surface area, average pore diameter and pore volume were determined by Brunauer Emmett and Teller (BET) method (Micromeritics ASAP 2020, USA). The surface area, average pore diameter and pore volume of the synthesized AgNPs were found to be 19.26 m^2/g, 16.1 nm and 0.11 cm^3/g respectively. Internal morphology of the AgNPs was analyzed using High resolution - transmission electron microscope (HR-TEM) (JEOL JEM 2100, USA). FTIR spectra was studied for unloaded and loaded AgNPs, to analyze the functional groups present in the AgNPs which are accountable for phenol removal by adsorption process. The crystalline nature of the AgNP is studied by XRD (Shimadzu, Japan). The surface structure of synthesized AgNPs and phenol sorbed AgNPs were also examined by SEM analysis (Jeol, USA). Elemental constituents of the composite were analyzed using energy dispersive X-ray spectroscopy (EDS). Thermo gravimetric analysis (TGA) for the synthesized AgNPs were also carried out.

2.5. Experimentation

Adsorptive removal of phenol was performed in Erlenmeyer flasks using the synthesized AgNPs based on the BBD given in Table 2. The 100 ppm phenol solution was taken in a 250 ml flask and the AgNPs were added. The solution was agitated in incubated shaker for specified time (3 h). Then the solution was centrifuged for 15 min at 10,000 rpm. The phenol concentration in the supernatant layer was analyzed in spectrophotometer (Shimadzu, Japan). The phenol uptake per unit mass of AgNPs (q, mg/g) is given by Eq.2:

Table 3
BBD and AMC Mediated AgNps yield.

Sl.No	A	B	C	D	AgNps yield (g)	
					Experimental	Predicted
1	1	-1	0	0	0.5	0.688
2	0	0	0	0	1.7	1.833
3	1	0	0	-1	2.1	2.154
4	0	0	-1	1	1.9	1.887
5	1	0	0	1	2.3	2.337
6	-1	-1	0	0	0.4	0.338
7	0	-0	1	1	2.0	2.037
8	0	1	0	1	2.3	2.358
9	1	1	0	0	0.4	2.554
10	0	0	1	0	2.0	1.508
11	1	0	0	0	2.3	1.833
12	0	0	1	0	2.5	2.358
13	0	10	1	-1	1.4	1.604
14	-1	-1	0	-1	1.8	0.458
15	0	1	0	0	2.5	1.804
16	-1	0	-1	-1	1.6	1.854
17	-1	0	0	1	0.6	1.837
18	0	0	0	-1	2.0	1.554
19	-1	1	-1	0	1.9	2.154
20	0	0	-1	0	1.8	1.858
21	0	0	0	0	2.0	1.833
22	1	0	-1	0	2.3	2.108
23	0	-1	0	1	0.5	0.342
24	0	-1	1	0	0.4	0.438
25	0	-1	-1	0	0.2	0.337
26	0	1	0	-1	1.7	1.775
27	0	1	1	0	2.0	1.954

Table 4
ANOVA for enhanced synthesis AgNps by AMC.

Source	Sum of Squares	df	Mean Square	F-value	P-value
Model	12.56	14	0.90	37.00	< 0.0001
A	0.91	1	0.91	37.44	< 0.0001
B	8.33	1	8.33	343.84	< 0.0001
C	7.500	1	7.500	0.31	0.5882
D	0.16	1	0.16	6.74	0.0234
AB	0.040	1	0.040	1.65	0.2231
AC	0.090	1	0.090	3.71	0.0780
AD	2.500	1	2.500	0.10	0.7536
BC	0.023	1	0.023	0.93	0.3543
BD	0.12	1	0.12	5.05	0.0441
CD	0.040	1	0.040	1.65	0.2231
A^2	0.083	1	0.083	3.44	0.0884
B^2	2.00	1	2.00	82.56	< 0.0001
C^2	0	1	0	0	1.0000
D^2	8.33	1	8.33	0.034	0.8560
Residual	0.29	12	0.024		
Lack of fit	0.24	10	0.024	1.05	0.5829
Pure error	0.047	2	0.023		
Cor total	12.85	26			

SD- 0.16; R^2- 0.9774; Mean- 1.62; Adj R^2- 0.9509; C.V.%9.60; Pred R^2- 0.8824; PRESS - 1.51; Adeq Precision- 19.103

$$q = \frac{(C_o - C_e)V}{m} \quad (2)$$

The phenol uptake at time t is given by Eq. (3):

$$qt = \frac{(C_o - C_t)V}{m} \quad (3)$$

where v – solution volume (L),

C_o – initial phenol concentration (mg/L),
C_e – equilibrium phenol concentration (mg/L),
C_t - phenol concentration at time t (mg/L)
m - mass of AgNPs (g).

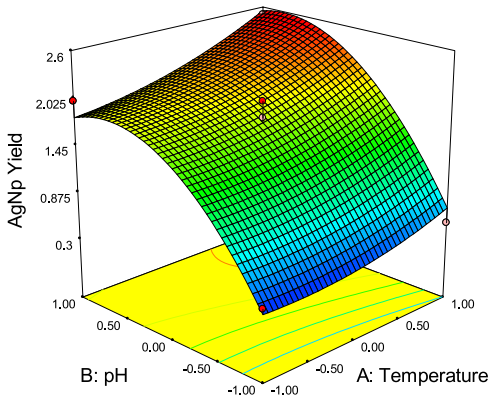


Fig. 1. pH & temperature interaction on AMC Mediated AgNps yield.

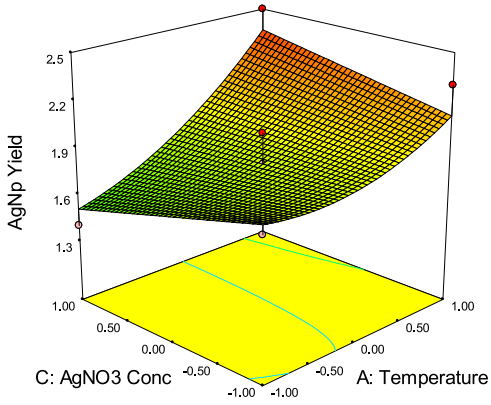


Fig. 2. $AgNO_3$ Concentration & temperature interaction on AMC Mediated AgNps yield.

3. Results and discussion

3.1. Enhancement of AgNPs synthesis

BBD based experimentation results for AgNp synthesis were presented in Table 3 along with the theoretically calculated AgNp. The correlation between AgNPs yield, response and the variables, temperature (A), pH (B), concentration of $AgNO_3$ (C), concentration of inoculum (D) is given by Eq. (4):

$$\text{AgNPs yield, g} = 1{\cdot}83 + 0{\cdot}284A + 0{\cdot}83B - 0.025\,C + 0{\cdot}12D + 0{\cdot}10AB + 0{\cdot}15AC - 0.075\,CE - 0.075\,BCE + 0.17\,BD + 0.10\,CD + 0{\cdot}13A^2 - 0{\cdot}61B^2 + 0.00\,C^2 + 0{\cdot}012D^2 \quad (4)$$

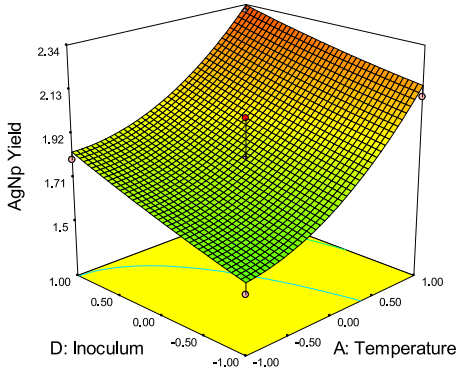


Fig. 3. Inoculum concentration & temperature interaction on AMC Mediated AgNps yield.

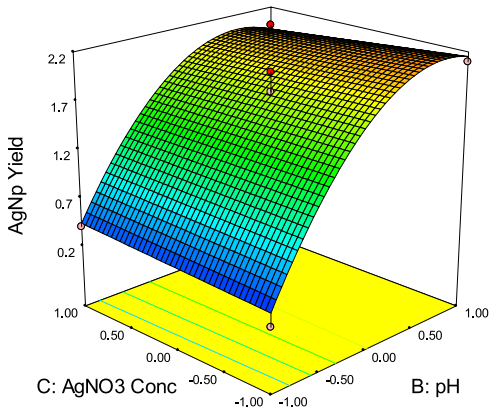


Fig. 4. $AgNO_3$ concentration & pH interaction on AMC Mediated AgNps yield.

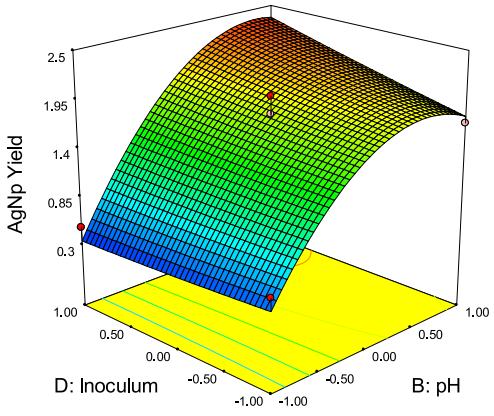


Fig. 5. Inoculum concentration & pH interaction on AMC Mediated AgNps yield.

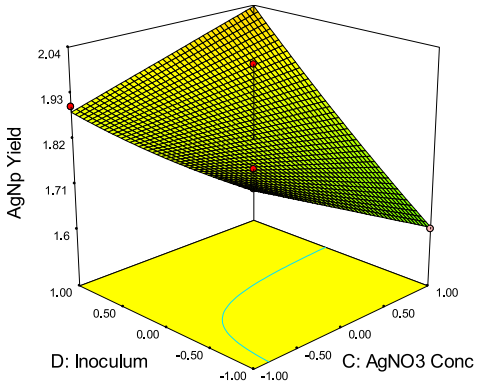


Fig. 6. Inoculum concentration & $AgNO_3$ concentration interaction on AMC Mediated AgNps yield.

The analysis of variance (ANOVA) results were tabulated in Table 4. F value of 37.00 specifies the importance of the model equation developed for AgNPs synthesis. The R^2 value of 0.9774, confirms that the model developed has predicted the experimental data well. The value of the Adj R^2 (0.9509) is also high. The Pred R^2 (0.8824) was found to be comparable with the Adj R^2. Low coefficient of variation (9.60), confirms the low value of difference between experimental and predicted yield of AgNPs. Adeq precision (19.103) shows good signal as this value should be greater than 4. The P value more than 0.05 for lack of fit indicates non significance and the model fitting becomes valid. The $P < 0.05$ shows the significance of the parameters. From the p values in ANOVA table, linear effect of temperature, pH, inoculum concentration, interactive effect of pH and inoculum concentration, and square effect of pH are identified as the highly significant factors for the synthesis of AgNPs.

The linear and interactive effects of factors on AgNP synthesis were investigated using the surface plots and they were shown in Figs. 1–6. The temperature effect on AgNP synthesis, is studied in the range of 30–90°C and it is depicted in Figs. 1, 2 and 3. From the figures, it is inferred that AgNP production increases with temperature and maximum AgNPs production occurs at 90 °C. Related studies have reported that the rate of formation of AgNps increases with increase in temperature (Ravichandran et al., 2011; Muthu Kumara Pandian et al., 2016).

The pH effect on AgNP production is studied between 5 and 9, and it is shown in Figs. 1, 4 and 5. From these figures, it is observed that the nanoparticles production is maximum at alkaline conditions (pH 8.6). Vanaja et al. (2014) and Bankar et al. (2010) concluded that acidic pH does not facilitate the formation of AgNps. In the alkaline range, number of functional groups available for the binding of silver are high (Ravichandran et al. 2011). Moreover, deactivation of biomolecules is reported to occur in acidic medium (Sathishkumar et al. 2009).

The effect of concentration of $AgNO_3$ concentration on AgNPs yield was studied between 1 and 3 mg/ml and the results were depicted in Figs. 2, 4 and 6. Synthesis of AgNps depends on the efficient conversion of $AgNO_3$ by various biomolecules present in the microbial inoculum (Rastogi and Arunachalam, 2013). It is found that the maximum AgNP formed at 3 mg/ml.

The effect of inoculum concentration was explored between 1 and 3 ml and the results were illustrated in Figs. 3, 5 and 6. From these surface plots, it was found that increase in inoculum concentration enhances the formation of Ag nanoparticles. The maximum AgNPs production occurs at 3 ml. A maximum production of 2.65 g/100 ml of AMC mediated AgNPs is synthesized at the optimum conditions: Temperature - 90 °C, pH-8.6, $AgNO_3$ concentration – 3 mg/ml and Inoculum concentration - 3 ml. From Table 3, it is observed that the maximum production of AgNPs is 2.5 g/100 ml whereas at optimum condition it is 2.65 g/100 ml. Hence, the production of AgNPs increased by 0.15 g/100 ml due to optimized conditions using RSM.

3.2. Analysis of UV-Visible Spectroscopy

The formation of AgNPs is physically confirmed by visualizing the change of color from pale white to dark brown. The color change is because of the surface plasmon resonance (Mie, 1908; Bhainsa and Souza, 2006). The AgNPs absorption spectrum is in the band of 350–450 nm (Kadir et al., 2005). The plasmon absorption band peak at 430 nm (Fig. 7) confirms the formation of AgNPs.

3.3. HRTEM analysis

High resolution transmission electron microscopy image of the synthesized AgNPs was used to inspect the inner surface morphology and size of the synthesized nanoparticle. Fig. 8 shows the TEM images of AgNP. Fig. 8a shows the TEM image of silver nanoparticles, it shows the well defined spherical nanoparticles with small agglomerations. The size of the prepared nanoparticles was below 100 nm in range. The selected area electron diffraction pattern (SAED) of AgNPs is depicted in Fig. 8b. it show the well crystalline nature of the prepared sample which is arise from the Bragg's diffraction plane of the face-centered cubic (fcc) crystalline structure of metallic silver. Also the SAED pattern depicts the 110 plane, these results are well coincide with the XRD results. These results were in good agreement with a related study (Anandalakshmi et al. 2016).

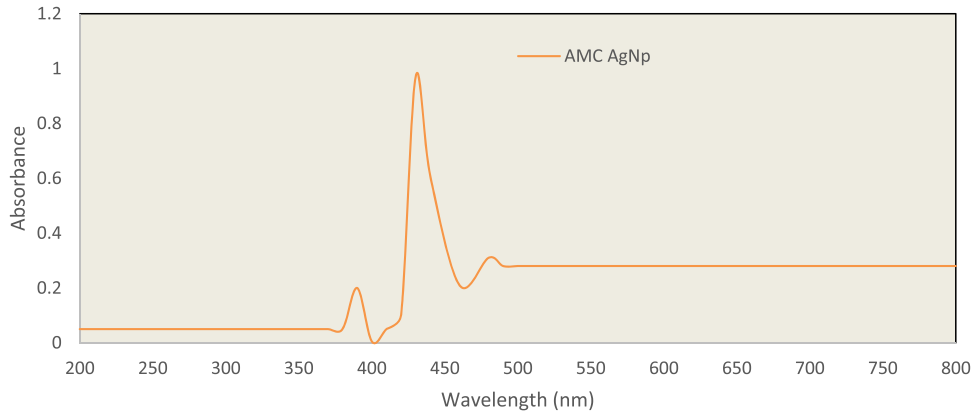


Fig. 7. UV-Visible Spectra of AMC Mediated AgNPs.

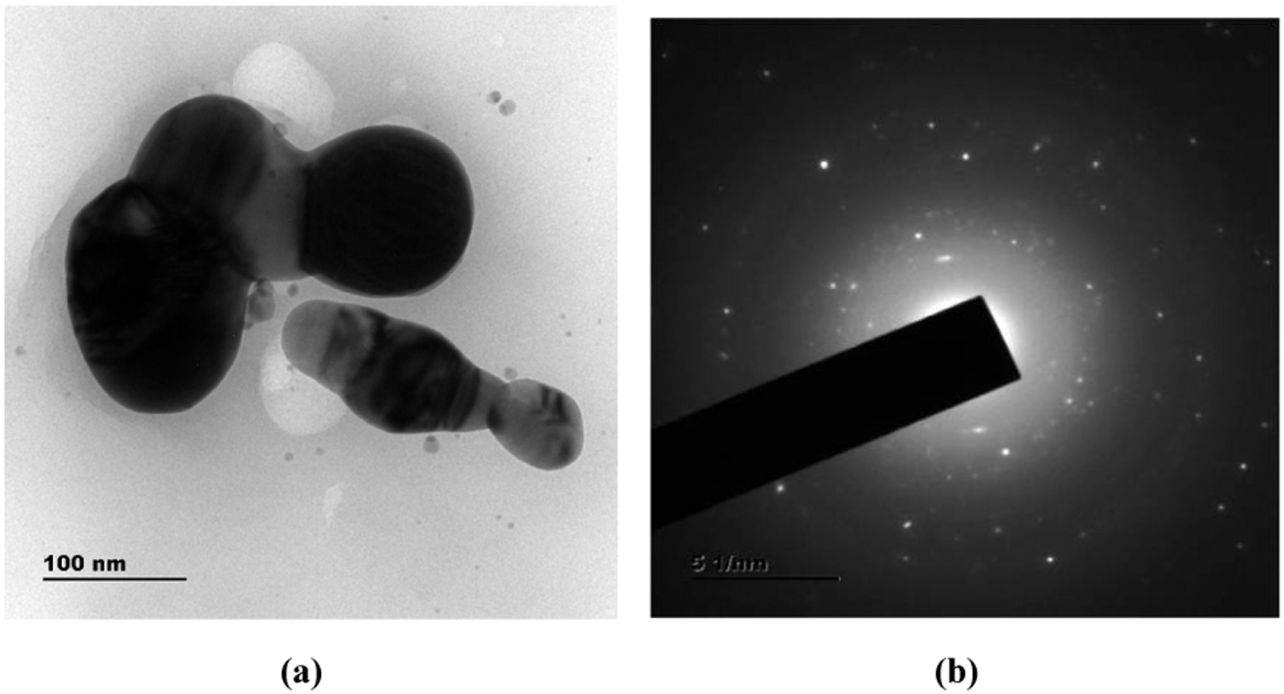


Fig. 8. (a) HRTEM image (b) SAED of synthesized silver nanoparticles.

3.4. Thermo – Gravimetric Analyses (TGA)

The different steps in the thermo gravimetric analysis of synthesized AgNPs, conducted in the temperature range of room temperature to 800 °C, were presented in Fig. 9. From the analysis, a meagre weight loss of 1.73% was observed till 225 °C. It shows the stability of the synthesized nanoparticles at low temperature range. In the temperature range of 225–450 °C, a drop in weight loss of 20.12% occurs. This may be due to evaporation of water and organic components present in the nanoparticles. Studies on silver nano particles reported similar observations (Majeed Khan et al., 2011).

3.5. Removal of phenol using the AgNPs

Phenol adsorption by AgNPs were performed based on BBD and the results were given in Table 5 along with the predicted phenol removal. The relationship between removal of phenol and process variables is given by Eq. (5):

$$\text{Removal of phenol} = 81{\cdot}33 - 3{\cdot}75A + 19{\cdot}63B + 5{\cdot}12\,C + 4{\cdot}75AB - 3{\cdot}75AC - 1{\cdot}00\,BCE - 6{\cdot}17A^2 - 21{\cdot}42B^2 - 3{\cdot}92\,C^2 \quad (5)$$

where A - pH, B - temperature ºC and C- nanoparticle dosage g/100 ml.

Table 6 shows the ANOVA for phenol removal using AgNPs. The significance of model is confirmed by F value (33.73). The R^2 value of 0.9838, confirms the model fit to the experimental data. A low CV (6.50), and high Adeq precision value (17.013) indicates the aptness of statistical tool. In this work, B, C, A^2 and B^2 were identified as the significant factors for the removal of phenol. This denotes that the linear effects of temperature and nanoparticle dosage and square effects of pH and temperature were the most important factors.

The pH effect on adsorption of phenol was presented in Figs. 10 and 11. The maximum percentage of phenol removal is observed at a pH of 5.8. The phenol removal depends on solution pH, which affects the AgNPs surface charge, degree of ionization and phenol speciation. From Figs. 10 and 11, it is observed that when the pH is increased from 3 to 6, the removal of phenol increases. Further increase in pH decreases the phenol removal. The decrease in phenol removal at higher pH by AgNps is well explained in literature (Muthu Kumara Pandian et al., 2016). Similar results are reported in other related studies (Asmaly et al., 2015,

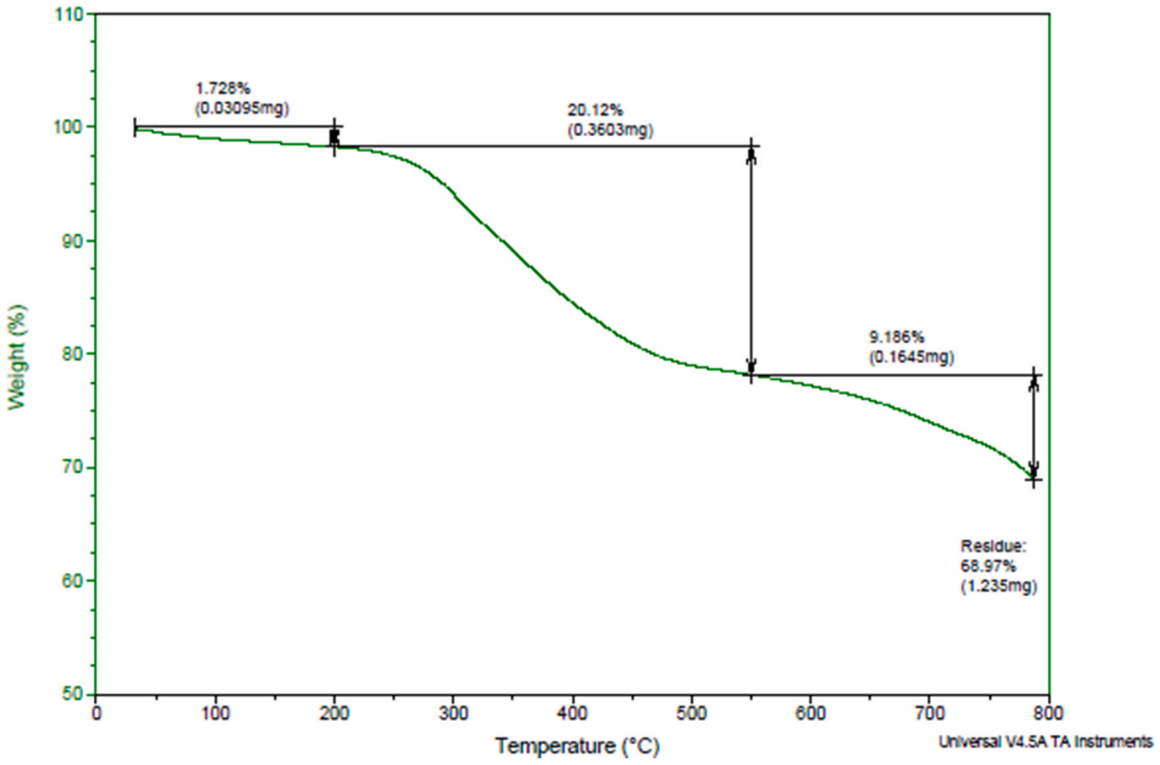


Fig. 9. TGA for synthesized silver nanoparticle.

Table 5
BBD and Phenol Removal results Using AMC Mediated AgNps.

Run Order	A	B	C	% Phenol removal	
				Experimental	Predicted
1	-1	-1	0	45.38	42.625
2	1	0	1	73.19	68.875
3	0	0	0	79.28	81.333
4	1	-1	0	25.57	25.625
5	0	-1	1	39.85	42.500
6	1	0	-1	65.52	66.125
7	1	1	0	72.43	74.375
8	-1	0	1	85.38	83.875
9	0	1	1	78.71	79.750
10	0	0	0	82.42	81.333
11	-1	1	0	73.26	72.375
12	0	1	-1	75.19	71.500
13	0	0	0	83.35	81.333
14	0	-1	-1	32.75	30.250
15	-1	0	-1	62.52	66.125

Table 6
ANOVA for Removal of Phenol Using AMC Mediated AgNps.

Source	Sum of Squares	df	Mean Square	F-value	P-value
Model	5337.82	9	5337.82	33.73	0.0006
A	112.50	1	112.50	6.40	0.0526
B	3081.12	1	3081.12	175.23	< 0.0001
C	210.13	1	210.13	11.95	0.0181
AB	90.25	1	90.25	5.13	0.0728
AC	56.25	1	56.25	3.20	0.1337
BC	4.00	1	4.00	0.23	0.6535
A^2	140.41	1	140.41	7.99	0.0369
B^2	1693.56	1	1693.56	96.32	0.0002
C^2	56.64	1	56.64	3.22	0.1326
Residual	87.92	5	17.58		
Lack of fit	79.25	3	26.42	6.10	0.1442
Pure error	8.67	2	4.33		
Cor total	5425.73	14			

Std. Dev.- 4.19; R^2- 0.9838; Mean- 64.53; Adj R^2- 0.9546;
C.V.%- 6.50; Pred R^2- 0.7627; PRESS- 1287.50; Adeq Precision- 17.013

Anisuzzaman et al., 2016).

The effect of temperature on removal of phenol is studied between 30°C and 60 °C and the outcome was depicted in Figs. 10 and 12. From these figures it was found that the sorption of phenol is high in the temperature range of 30°C to 35°C and 34 °C is the optimum temperature for maximum phenol removal. The decrease in phenol adsorption at higher temperature is because of texture modification in the AgNPs and a reduction in the adsorption capacity due to AgNps deterioration (Volesky, 2003).

The effect of nanoparticles dosage on phenol removal is studied between 0.1 and 0.9 g/100 ml and the results were shown in Figs. 11 and 12. The phenol adsorption is governed by the availability of surface sorption sites in the sorbent (Karimi et al., 2012). As AgNPs dose increases, the sorption site available for phenol increases, which facilitates higher removal of phenol. Maximum removal of phenol was obtained at sorbent dosage of 0.9 g/100 ml. At the optimum conditions, maximum

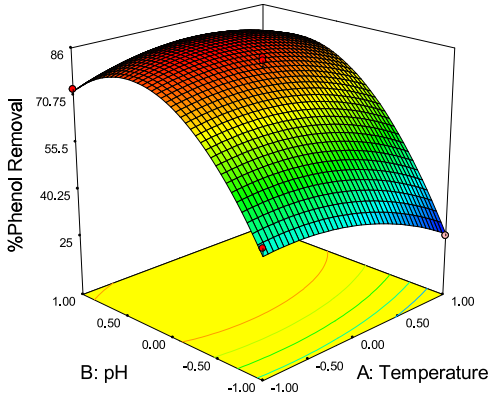


Fig. 10. pH and Temperature interactions on removal of Phenol.

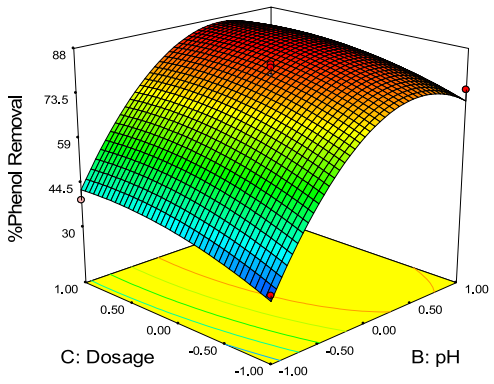


Fig. 11. pH and AgNps dosage interactions on removal of Phenol.

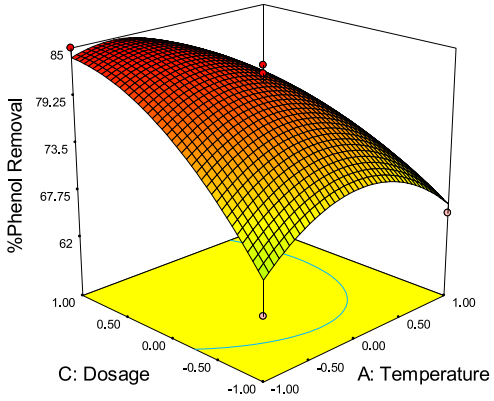


Fig. 12. Temperature and AgNps Dosage interactions on removal of Phenol.

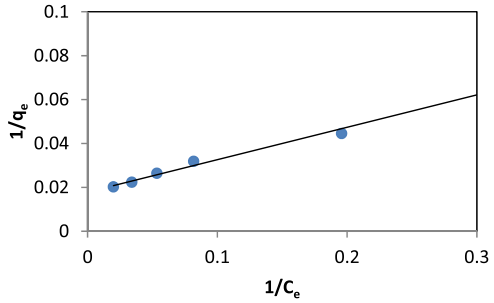


Fig. 13. Langmuir plot for Phenol removal using AMC mediated AgNp.

phenol removal of 87.65% was achieved. As shown in Table 5, the removal of phenol under optimal conditions was found to be 2% more than the value obtained at unoptimized conditions.

3.6. Equilibrium study

The mechanism of phenol adsorption by AgNPs, was studied using, Langmuir, Freundlich and Dubinin-Radushkevich (D-R) isotherms.

The Langmuir isotherm (Langmuir, 1916) is given by Eq. (6):

$$\frac{1}{q_e} = \frac{1}{q_m b C_e} + \frac{1}{q_m} \tag{6}$$

where q_m - Adsorption capacity (mg/g)

q_e - Equilibrium phenol concentration on the sorbent (mg/g)
C_e - Equilibrium concentration of phenol in the solution (mg/L) and

Table 7
Isotherm Model Parameters for the Sorption of Phenol Using AMC Mediated AgNp.

Isotherm	Parameters	AMC Mediated AgNp
Langmuir	q_{max}	56.1797 mg/g
	B	0.1205 l/mg
	R^2	0.9969
Freundlich	K_f	9.3282
	$1/n$	0.4583
	R^2	0.9578
D-R	q_{max}	39.0873 mg/g
	B	1.3835 mol^2/kJ^2
	E	0.6011 kJ/mol
	R^2	0.8757

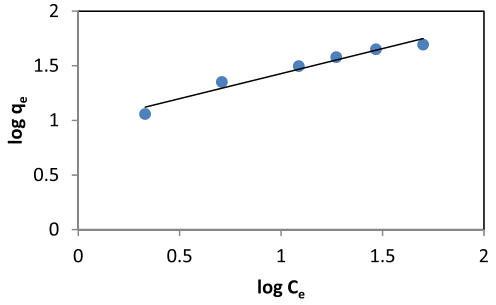


Fig. 14. Freundlich isotherm plot for removal of Phenol using AMC mediated AgNp.

b is the Langmuir sorption constant (l/mg) related to the free energy of sorption.

Fig. 13 shows the Langmuir plots for the sorption of phenol onto AgNP. The constants q_m and b were estimated and given in Table 7. High values of q_{max} and R^2 (0.9295) shows that AgNP as a potential sorbent for phenol removal.

The Freundlich isotherm (Freundlich, 1906) is given by Eq. (7):

$$\log q_e = \log K_f + \frac{1}{n} log C_e \tag{7}$$

where K_f - Sorption capacity constant.
$1/n$ - Empirical parameter.

Fig. 14 shows Freundlich isotherm for the adsorption of phenol by AgNPs. The calculated parameters were given in Table 7. For a good sorption, the 1/n value should be between 0 and 1. A value of 0.2812 favors phenol sorption by AgNPs.

The D-R isotherm equation (Dubinin, 1960) is given by Eq. (8):

$$\ln q_e = \ln q_m - \beta \epsilon^2 \tag{8}$$

where q_m – maximum uptake of phenol (mg/g)

β - Activity coefficient (mol^2/kJ^2) and
ϵ - Polanyi potential (given by Eq. (9))

$$\epsilon = RT \ln\left[1 + \frac{1}{C_e}\right] \tag{9}$$

R - 8.314 X 10^{-3} kJ/mol K
T - Temperature (K)

The mean free energy of sorption per molecule of sorbate (E) is found by Eq.(10):

$$E = \frac{1}{\sqrt{2\beta}} \tag{10}$$

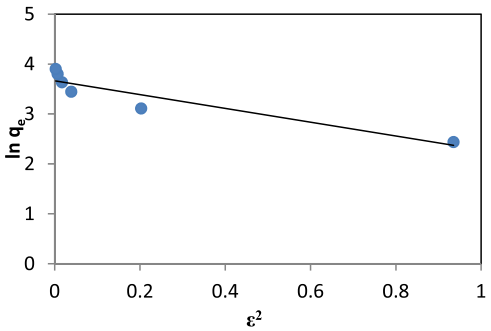


Fig. 15. D-R isotherm plot for removal of Phenol using AMC mediated AgNp.

Table 8
Various Sorbents and their Sorption Capacities for removal of Phenol.

Sorbent	Sorption capacity	Reference
Palm seed coat	18.3 mg/g	Rengaraj et al. 2002
Coir pith	48.31 mg/g	Namasivayam and Kavitha, 2006
Nut Shell of *Sterculia alata*	2.8 mg/g	Kaustubha et al. 2006
Almond Shell	10.4 mg/g	Santos et al. 2008
Oil palm empty fruit bunch	4.86 mg/g	Hameed et al. 2009
Hemidermus indicus roots	16.10 mg/g	Srihari and Ashotosh Das, 2009
Porous clay	14.5 mg/g	Gayatri, Ahmaruzzaman, Md., 2010
Activated carbon	39 mg/g	Jolanta et al. 2012
Cereal byproduct	11.45 mg/g	Sihem, et al. 2012
Carbonized saw dust	0.0221 mg/g	Larous and Meniai, 2012
Sodium zeolite	13.051 mg/g	Saravanakumar and Kumar, 2013
Sugarcane bagasse AC	35.71 mg/g	Karunarathne and Amarasinghe, 2013
Olive mill waste	24.4 mg/g	Abdelkreem, 2013
Rhassoul	25 mg/g	Hamdaoui et al., 2018
Rice straw	5.780 mg/g	Sarker and Fakhruddin, 2017
Pine fruit shells	26.738 mg/g	Mohammed et al. 2018
Organo-functional biochar	37.66 mg/g	Mingliang et al. 2019
Hematite	16.17 mg/g	Dehmani et al. 2020
AC from olive husk	9.039 mg/g	Hamadneh et al. 2020
Layered Double Hydroxide (LDH) clay	12 mg/g	Tabana et al. 2020
Oil palm biochar	49.74 mg/g	Lawal et al. 2020
AMC mediated AgNp	56.17 mg/g	Present study

The D-R constants, β and q_m were calculated from the plot (Fig. 15) and presented in Table 7. The E value less than 8 kJ/mol (Table 7), specifies that the phenol adsorption is a physical process. The satisfactory representation of isotherm experiments by Langmuir isotherm validates the occurrence of single layer adsorption of phenol on the surface of silver nanoparticles. Surface attachment on a specific active site could be the mechanism involved and justified through the presence of surface functional groups.

3.7. Comparison of uptake

The uptake of phenol by AgNPs is compared with the other sorbents for phenol removal and it is given in Table 8. The sorbent synthesized in this study, AMC mediated AgNp, is found to be very effective with comparatively higher phenol uptake (56.17 mg/g) and suitable for phenol removal.

3.8. Sorption kinetics

The kinetics of phenol adsorption by AgNPs is studied by pseudo first order (PFO), pseudo second order (PSO) and intra particle diffusional (IPD) models.

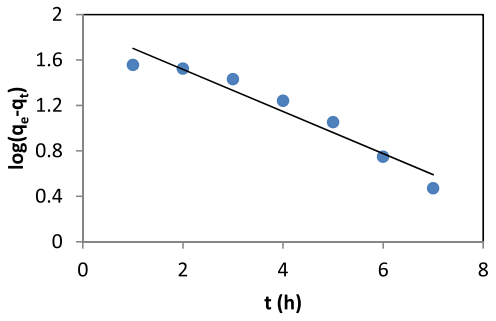


Fig. 16. Pseudo first order model for removal of Phenol using AMC mediated AgNp.

Table 9
Kinetic Model Parameters for Removal of Phenol Using AMC Mediated AgNp.

Kinetic Model	Parameters	Values
PFO	K_1	0.4269
	R^2	0.9380
PSO	K_2	0.0001
	R^2	0.6466
IPD	K_{id}	22.446
	R^2	0.9750

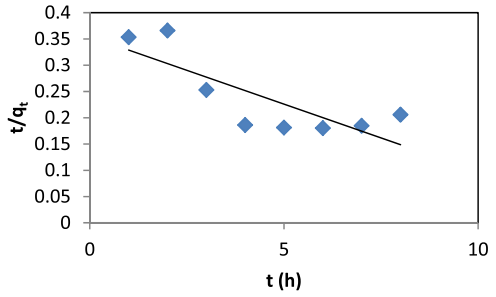


Fig. 17. Pseudo second order model for removal of Phenol using AMC Mediated AgNp.

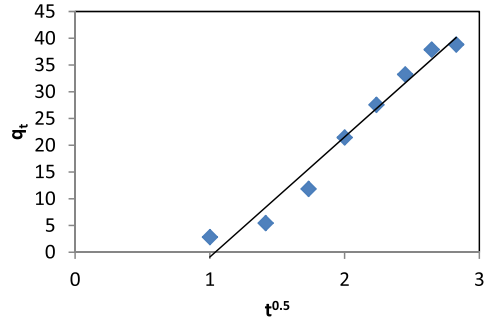


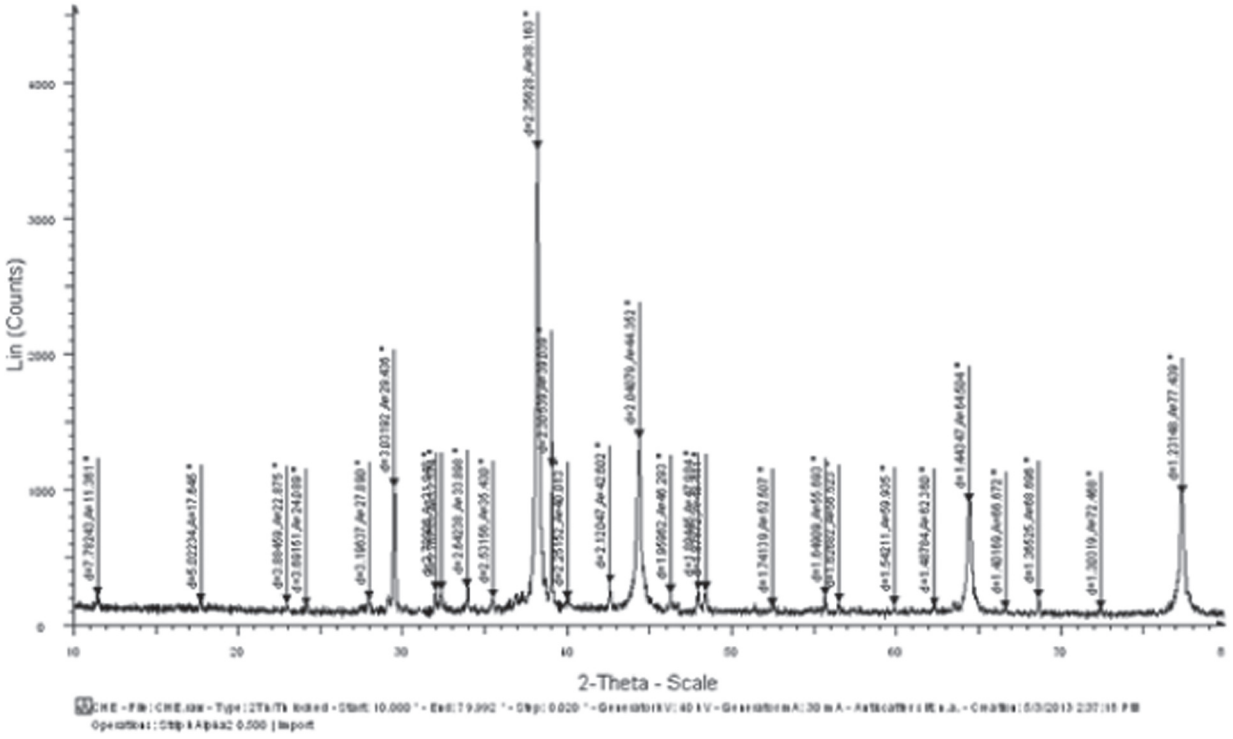
Fig. 18. Intraparticle diffusion model for removal of Phenol using AMC mediated AgNp.

The PFO model (Ho, 2004) is given by Eq. (11):

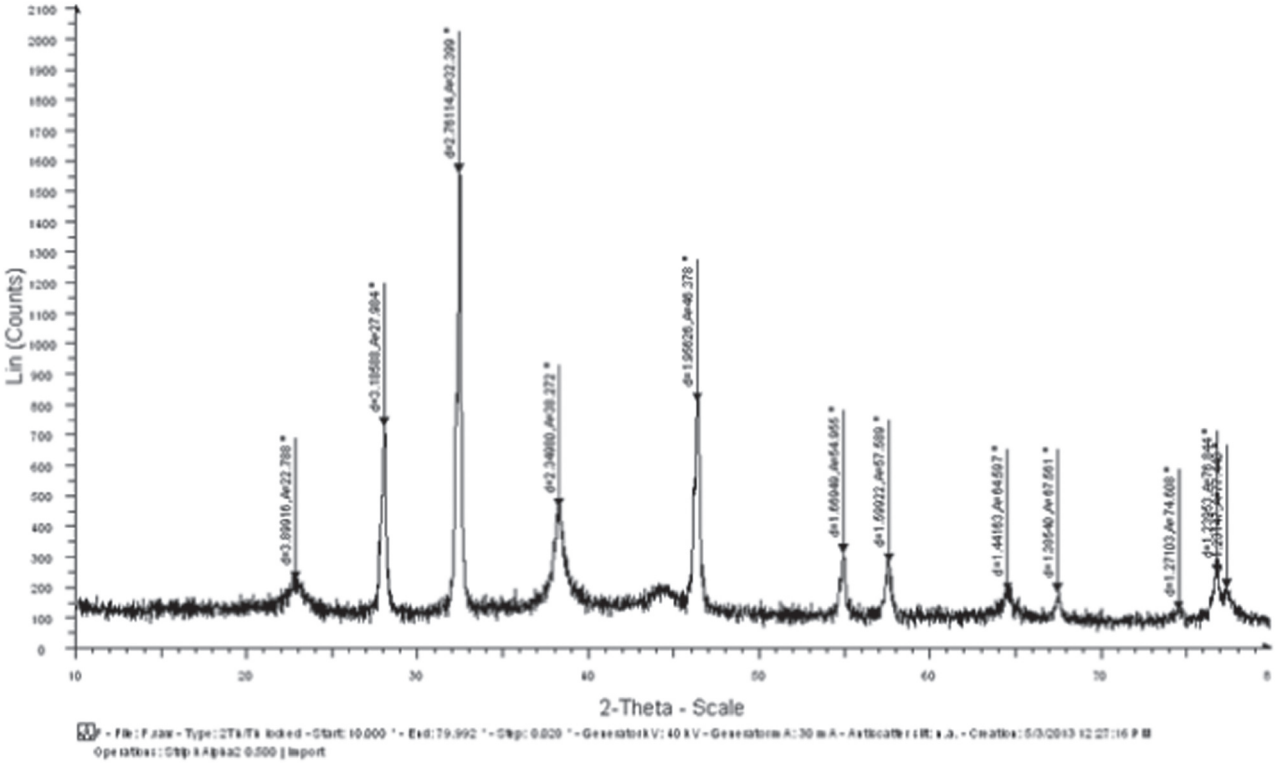
$$\log(q_e - q_t) = \log q_e - \frac{K_1}{2.303} t \quad (11)$$

where K_1 - rate constant of the pseudo first order model (min^{-1}). The value of K_1 is evaluated (Fig. 16) and it was reported in Table 9.

The PSO model (Ho, McKay, 1999) is given by Eq. (12):



(a)



(b)

Fig. 19. a. XRD Spectra of AgNP before sorption. b. XRD Spectra of AgNP after phenol adsorption.

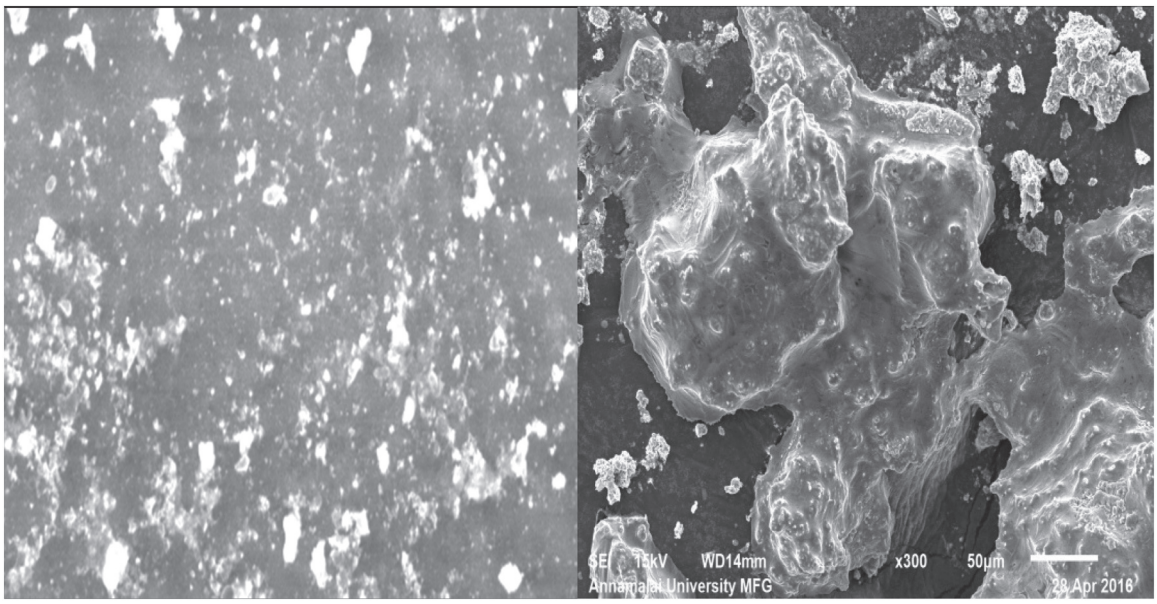


Fig. 20. a. AgNP before Phenol Sorption b. AgNP after Phenol Sorption.

$$\frac{t}{q_t} = \frac{1}{K_2 q_e^2} + \frac{1}{q_e} t \tag{12}$$

where K_2 (g/mg min) – PSO rate constant. The pseudo second order rate constant (K_2) is estimated from Fig. 17 and tabulated in Table 9 along with R^2 values. The R^2, value was low for pseudo second order model.

IPD model (Weber and Morris, 1963) is given by Eq. (13):

$$q_t = K_{id} t^{0.5} + C \tag{13}$$

Where K_{id} – IPD rate constant (mg/g $min^{0.5}$) and C - intercept. The constants were calculated using Fig. 18 and the values were summarized in Table 9. A high R^2 value show fitness of the IPD model for phenol sorption using AgNPs.The suitability of the kinetic data to intra-particle diffusion model confirmed that diffusion through pores is the slowest and rate-determining step. In addition, this model validates the instantaneous nature of adsorption process.

3.9. X-ray Diffraction Analysis

The crystalline nature of the materials were observed by XRD analysis. The crystalline material shows peaks while the non-crystalline show a hallow observation (Ramesh et al., 2014). The XRD analysis of synthesized AgNPs (raw and phenol sorbed) were shown in Fig. 19 a and b. From these figures, it was inferred that the high-pitched diffraction peaks which corresponds to $2\Theta = 29.436$, 38.163 and 44.352 with d spacing of 3.03 Å, 2.35 Å and 2.040 Å and 27.084, 38.272 and 46.378 with d spacing of 3.185 Å, 2.34 Å and 1.95 Å, respectively confirms the crystallinity. Also in Fig. 19 b, the peaks were decreased when compared to Fig. 19 a. This change in crystallinity of the AgNPs was attributed to the adsorption phenol onto AgNPs.

3.10. Scanning Electron Microscopy

SEM was employed to analyze the changes in the surface morphological structure of synthesized AgNPs, before and after the sorption of phenol. In the SEM image (Fig. 20a), the synthesized AgNPs, were easily identified and were mostly individual and spherical. After the sorption of phenol, the size varies from 100 to 500 nm approx. This may be due to the agglomeration of particles during adsorption (Fig. 20b). Also the surface of AgNPs were rough prior to phenol adsorption and found to be even after the sorption of phenol.

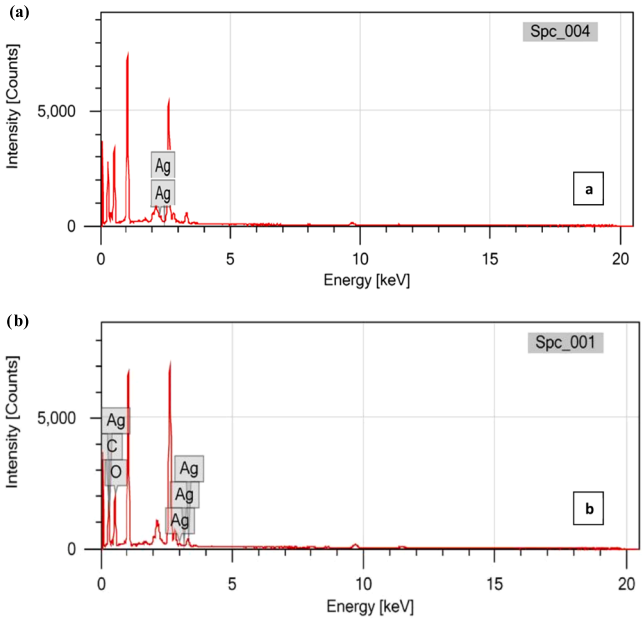


Fig. 21. EDS profile for synthesized AgNPs (a) before sorption (b) After phenol sorption.

Electron dispersion spectroscopy (EDS) spectra of AgNPs were shown in Fig. 21 a and b. A strong peak (Fig. 21 a) was observed at 3 KeV which is typical for absorption of metallic silver nanoparticles. The absence of other elements confirmed the purity of the synthesized silver nanoparticles. The results were in accordance with related study (Anandalakshmi et al. 2016). As shown in Fig. 21 b, the presence of elements, namely C, H and O, confirms the adsorption of phenol.

3.11. FTIR analysis

The sorbed and unsorbed AgNps were analyzed by means of FTIR

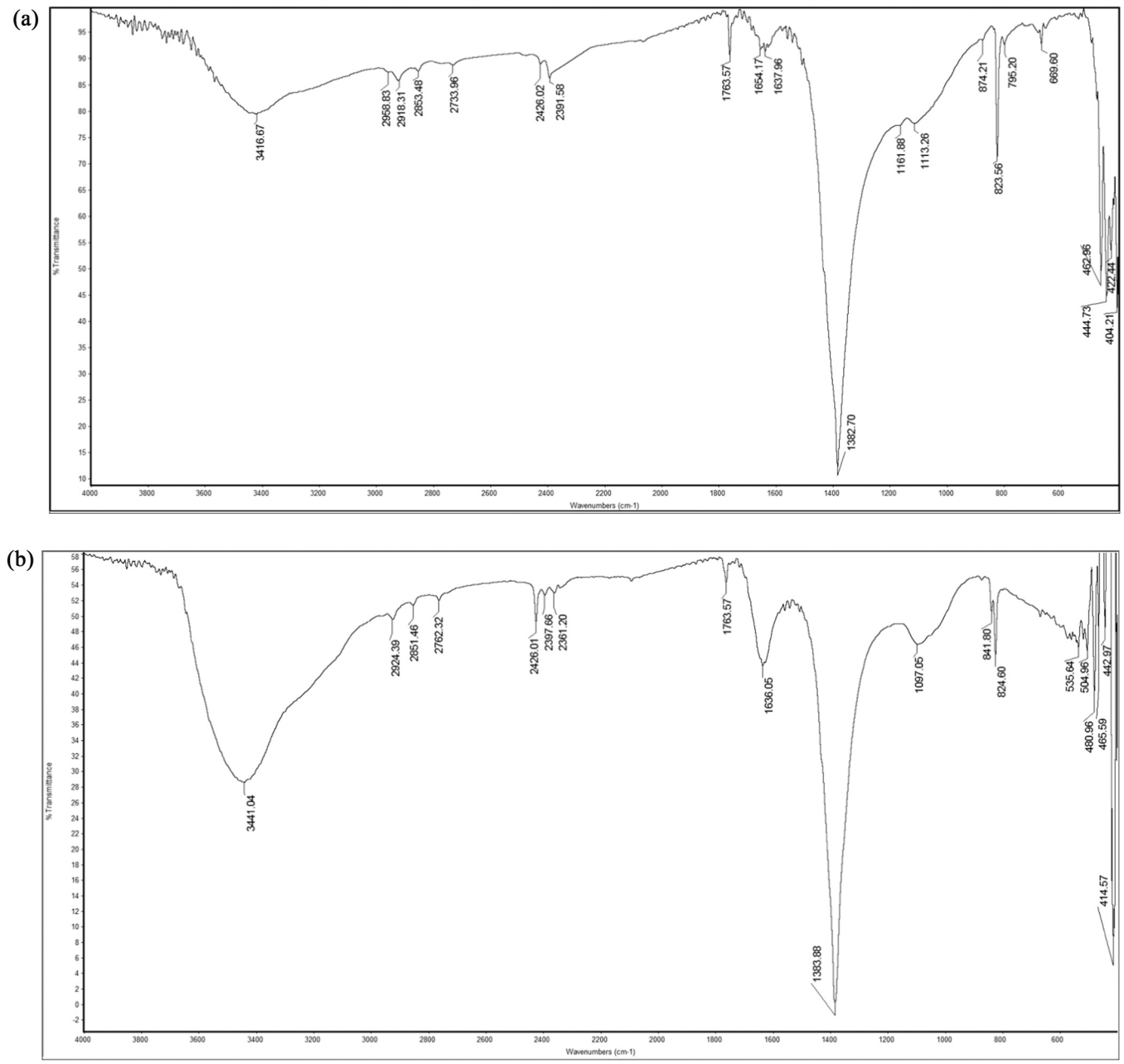


Fig. 22. a. FTIR Spectra of AMC mediated AgNps - Before Sorption of Phenol. b. FTIR Spectra of AMC mediated AgNps - After Sorption of Phenol.

(Fig. 22 a and 22 b) to investigate about the presence of functional groups which are responsible for phenol adsorption. The FTIR spectrum of the AgNPs is investigated in the spectral range between 4000 and 400 cm^{-1}. The figure show 5 major zones and the assigned corresponding functional groups were given in Table 10. The FTIR spectrum displays broad absorption band between 3500 and 3000 cm^{-1} because of O–H stretching, H- bonded alcohols and phenol groups. The primary and secondary amine NH band along with primary amine CN stretching vibrations of the proteins were depicted at1150 and 480 cm^{-1} respectively.

3.12. Desorption and regeneration of AgNPs

In adsorption process, regeneration of used adsorbent is necessary to reduce the cost of sorption process and ensure the reusability of the sorbent. Desorption of phenol from the loaded AgNPs is performed using 1 M NaOH. The reuse of sorbent is examined by conducting experiments repeatedly for eight cycles. In the first cycle, 85% of phenol is removed. Then, the used sorbent is treated with NaOH which resulted in 95% stripping of phenol. The percentage removal of phenol is around 85% till fifth cycle. After fifth cycle the percentage removal of phenol diminished. The decrement in sorption efficiency may be due to loss of sorbent or deterioration of AgNP. The results suggest that AgNP is effectively utilized and can be reused for the sorption of phenol without losing its efficiency for five cycles.

4. Conclusion

This study has demonstrated the successful application of biologically mediated silver nanoparticles for the efficient removal of phenol under diversified conditions. The synthesis of silver nanoparticles was maximized through response surface methodology based tools. The BBD based statistical methods helped to identify the most influencing factors influencing the adsorption of phenol onto silver nanoparticles. The

Table 10
FTIR results of AMC Mediated AgNps for Before and After Removal of Phenol.

Wavelength Range (cm^{-1})	AMC Mediated AgNps			Assignment
	Before Sorption	After Sorption	Differences	
3500 – 3000	3416.67	3431.04	+ 14.37	Bonded–OH groups
2900 – 2800	2958.83	–	+ 2958.83	CH stretching
	2918.31	2924.39	+ 6.08	
	2853.48	2851.46	-2.02	
	2733.96	2762.32	+ 28.36	
	2426.02	2426.01	+ 0.01	
	2391.58	2397.66	+ 6.08	
1740 – 1680	1763.57	1763.57	–	C=Ocarbonyl
	1654.17	–	-1654.17	groups
	1637.96	1636.05	-1.91	
1500 – 1300	1382.70	1383.88	+ 1.18	C-O stretch
1150 – 850	1161.88	–	-1161.88	$-PO_4^{3-}$ stretching
	1113.26	1097.05	-16.21	
	874.21	841.80	-32.41	
	823.56	824.60	+ 1.04	
	795.20	–	-795.20	
650 – 480	669.60	535.64	-133.96	N-containing
	–	504.96	+ 504.96	bioligands
	462.96	465.59	+ 2.63	
	444.73	442.97	-1.76	
	422.44	414.57	-7.87	
	404.21	–	-404.21	

favourable properties of silver nanoparticles to be used as an efficient nano-sorbent was proved through higher surface area, nano-scale pore diameter (16.1 nm), enhanced pore volume (0.11 cm^3/g), active functional groups, enhanced thermal stability and organized crystal structure. The relationship between removal of phenol and process variables were identified to understand the important influencing factors. The isotherm studies shows that the Langmuir model suited well the phenol sorption by AgNPs when compared to Freundlich and Dubinin-Radushkevich isotherm models. The experimental data were fitted to pseudo-first order, pseudo-second order and intra-particle diffusion models and intra-particle diffusion is identified as rate controlling mechanism.

CRediT authorship contribution statement

A. Muthu Kumara Pandian: Conceptualization, Methodology, Investigation, Validation, Writing - original draft. **M. Rajasimman:** Conceptualization, Methodology, Formal analysis, Writing - review & editing. **N. Rajamohan:** Resources, Writing - review & editing. **S. Varjani:** Characterization, Writing - review & editing. **C. Karthikeyan:** Conceptualization, Formal analysis, Writing - review & editing Supervision.

Declaration of Competing Interest

The authors declare that they have no known competing financial interests or personal relationships that could have appeared to influence the work reported in this paper.

References

Abdelkreem, M., 2013. Adsorption of phenol from industrial wastewater using olive mill waste. APCBEE Procedia 5, 349–357.

Anandalakshmi, K., Venugobal, J., Ramasamy, V., 2016. Characterization of silver nanoparticles by green synthesis method using *Pedalium murex* leaf extract and their antibacterial activity. Appl. Nano Sci. 6, 399–408.

Anisuzzaman, S.M., Collin, G., Krishnaiah, D., Bono, A., Suali, E., Abang, S., Fai, L.M., 2016. Removal of chlorinated phenol from aqueous media by guava seed (Psidium guajava) tailored activated carbon. Water Resour. Ind. 16, 29–36.

Asmaly, H.A., Abussaud, B., Ihsanullah, Saleh, T.A., Gupta, V.K., Atieh, M.A., 2015. Ferric oxide nanoparticles decorated carbon nanotubes and carbon nanofibers: from synthesis to enhanced removal of phenol. J. Saudi Chem. Soc. 19, 511–520.

Bankar, A., Joshi, B., Kumar, A.R., Zinjarde, S., 2010. Banana peel extract mediated novel route for the synthesis of silver nanoparticles. Colloids Surf. A 368 (1), 58–63.

Bansal, V., Ramanathan, R., Bhargava, S.K., 2011. Fungus mediated biological approaches towards green synthesis of oxide nanomaterials. Aust. J. Chem. 64, 279–293.

Bhainsa, K.C., Souza, S.F.D., 2006. Extracellular biosynthesis of silver Nanoparticles using the fungus Aspergillus fumigatus. Colloids Surf. B 47, 160–164.

Dehmani, Y., Al rashdi, A.A., LGaz, H., Lamhasni, T., Abouarnadasse, S., Chung, I.M., 2020. Removal of phenol from aqueous solution by adsorption onto hematite (α-Fe_2O_3): mechanism exploration from both experimental and theoretical studies. Arab. J. Chem. 13, 5474–5486.

Dubinin, M.M., 1960. The potential theory of adsorption of gases and vapors for adsorbents with energetically non-uniform surfaces. Chem. Rev. 60, 235–266.

Freundlich, H.M.F., 1906. Over the adsorption in solution. J. Phys. Chem. 57, 385–470.

Gayatri, Laxmi, Ahmaruzzaman, Md, S., 2010. Adsorption technique for the removal of phenolic compounds from wastewater using low-cost natural adsorbents. Assam. Univ. J. Sci. Technol. Phys. Sci. Technol. 5 (2), 156–166.

Hamadneh, I., Abu-Zurayk, R.A., Al-Dujaili, A.H., 2020. Removal of phenolic compounds from aqueous solution using $MgCl_2$-impregnated activated carbons derived from olive husk: the effect of chemical structures. Water Sci. Technol. 81 (11), 2351–2367.

Hamdaoui, M., Hadri, M., Bencheqroun, Z., Draoui, K., Nawdali, M., Zaitan, H., Barhoun, A., 2018. Improvement of phenol removal from aqueous medium by adsorption on organically functionalized Moroccan stevensite. J. Mater. Environ. Sci. 9, 1119–1128.

Hameed, B.H., Tan, I.A.W., Ahmad, A.L., 2009. Preparation of oil palm empty fruit bunch based activated carbon for removal of 2,4,6-trichlorophenol: Optimization using response surface methodology. J. Hazard. Mater. 164, 1316–1324.

Ho, Y.S., 2004. Citation review of Lagergen Kinetic rate equation on adsorption reactions Scientometrics, 59 (1), 171–177.

Ho, Y.S., McKay, G., 1999. Pesudo-second order model for sorption processes. Process Biochem. 34, 451–465.

Ihsan, H.D., 2013. Removal of phenol from industrial wastewater using sawdust. Int. J. Eng. Sci. 3, 25–31.

Islam, M.A., Jacob, M.V., Antunes, E., 2021. A critical review on silver nanoparticles: From synthesis and applications to its mitigation through low-cost adsorption by biochar. J. Environ. Manag. 281, 111918.

Jolanta, B., Gabriela, K., Malwina, T., 2012. The removal of phenols from wastewater through sorption on activated carbon. Archit. Civ. Eng. Environ. 2, 89–94.

Kadir, A., Joseph, R.L., Chris, D.G., 2005. Rapid deposition of triangular silver nanoplates on planar surfaces: application to metal-enhanced fluorescence. J. Phys. Chem. 109 (B), 6247–6251.

Karimi, H., Mousavi, S., Sadeghian, B., 2012. Silver nanoparticle loaded on activated carbon as efficient adsorbent for removal of methyl orange. Indian J. Sci. Technol. 5, 2346–2353.

Karunarathne, H.D.S.S., Amarasinghe, B.M.W.P.K., 2013. Fixed Bed Adsorption Column Studies for the Removal of Aqueous Phenol from Activated Carbon Prepared from Sugarcane Bagasse. Energy Procedia 34, 83–90.

Kaustubha, M., Das, D., Biswas, M.N., 2006. Preparation and characterization of activated carbons from Sterculia alata nutshell by chemical activation with zinc chloride to remove phenol from wastewater. Adsorption 12, 119–132.

Langmuir, I., 1916. The adsorption of gases on plane surface of glass, mica and platinum. J. Am. Chem. Soc. 40, 1361–1368.

Larous, S., Meniai, A.H., 2012. The use of sawdust as by product adsorbent of organic pollutant from wastewater: adsorption of phenol. Energy Procedia Vol. 18, 905–914.

Lawal, A.A., Hassan, M.A., Ahmad Farid, M.A., Yasim-Anuar, T.A.T., Mohd Yusoff, M.Z., Zakaria, M.R., Roslan, A.M., Mokhtar, M.N., Shirai, Y., 2020. One-step steam pyrolysis for the production of mesoporous biochar from oil palm frond to effectively remove phenol in facultatively treated palm oil mill effluent. Environ. Technol. Innov. 18, 100730.

Majeed Khan, M.A., Kumar, S., Ahamed, M., Alrokayan, S.A., Alsalhi, M.S., 2011. Structural and thermal studies of silver nanoparticles and electrical transport study of their thin films. Nanoscale Res. Lett. 6, 434.

Mie, G., 1908. Contributions to the optics of turbid media especially colloidal metal solutions. Ann. Phys. 25, 377–445.

Mingliang, G., Xubin, W., Mingyi, D., Guodong, L., Guoqing, H., Jahangir, A.S.M., 2019. Adsorption analyses of phenol from aqueous solutions using magadiite modified with organo-functional groups: kinetic and equilibrium studies. Materials 12, 1–16.

Mittal, A.K., Bhaumik, J., Kumar, S., Banerjee, U.C., 2014. Biosynthesis of silver nanoparticles: Elucidation of prospective mechanism and therapeutic potential. J. Colloid Interface Sci. 415, 39–47.

Mohammed, N.A.S., Abu-Zurayk, R.A., Hamadneh, I., Al-Dujaili, A.H., 2018. Phenol adsorption on biochar prepared from the pine fruit shells: equilibrium, kinetic and thermodynamics studies. J. Environ. Manag. 226, 377–385.

Mukherjee, P., Ahmad, A., Mandal, D., Senapati, S., Sainkar, S.R., Khan, M.I., Parishcha, R., Ajaykumar, P.V., Alam, M., Kumar, R., Sastry, M., 2001. Fungus-mediated synthesis of silver nanoparticles and their immobilization in the mycelial matrix: a novel biological approach to nanoparticle synthesis. Nano Lett. 1, 515–519.

Muthu Kumara Pandian, A., Karthikeyan, C., Rajasimman, M., 2016. Isotherm and Kinetic Studies on nano-sorption of Malachite Green onto *Allium sativum* mediated synthesis of silver nano particles. Biocatal. Agric. Biotechnol. 8 (8), 171–181.

Namasivayam, C., Kavitha, D., 2006. IR, XRD and SEM studies on the mechanism of adsorption of dyes and phenols by coir pith carbon from aqueous phase. Microchem. J. 82 (1), 43–48.

Pishgar, R., Najafpour, G.D., Mousavi, N., Bakhshi, Z., Khorrami, M., 2012. Phenol biodegradation kinetics in the presence of supplimentary substrate. Int. J. Eng. Trans. B Appl. 25 (3), 181–191.
Rafique, M., Sadaf, I., Rafique, M.S., Tahir, M.B., 2017. A review on green synthesis of silver nanoparticles and their applications. Artif. Cells Nanomed. Biotechnol. 45 (7), 1272–1291.
Ramesh, K., Rajappa, A., Nandhakumar, V., 2014. IR, XRD and SEM studies on adsorption of methylene blue dye onto microwave assisted $ZnCl_2$ activated carbon prepared from *Delonix regia* PODS. Int. J. Curr. Res. Chem. Phram. Sci. 1 (4), 15–19.
Rastogi, L., Arunachalam, J., 2013. Green synthesis route for the size controlled synthesis of biocompatible gold nanoparticles using aqueous extract of garlic (Allium sativum). Adv. Mater. Lett. 4 (7), 548–555.
Ravichandran, V., Tiah, Z.X., Subashini, G., Terence, F.W.X., Eddy, F.C.Y., Nelson, J., Sokkalingam, A.D., 2011. Biosynthesis of silver nanoparticles using mangosteen leaf extract and evaluation of their antimicrobial activities. J. Saudi Chem. Soc. 15 (2), 113–120.
Rengaraj, S., Moon, S.H., Sivabalan, R., Arabindoo, B., Murugesan, V., 2002. Agricultural solid waste for the removal of organics: adsorption of phenol from water and wastewater by palm seed coat activated carbon. Waste Manag. 22 (5), 543–548.
Santos, L., Estevinho, B.N., Ribeiro, E., Alves, A., 2008. A preliminary feasibility study for pentachlorophenol column sorption by almond shell residues. Chem. Eng. J. 136 (2), 188–194.
Saravanakumar, K., Kumar, A., 2013. Removal of phenol from aqueous solution by adsorption using zeolite. Afr. J. Agric. Res. 8 (23), 2965–2969.
Sarker, N., Fakhruddin, A.N.M., 2017. Removal of phenol from aqueous solution using rice straw as adsorbent. Appl. Water Sci. 7, 1459–1465.
Sathishkumar, M., Sneha, K., Won, S.W., Cho, C.W., Kim, S., Yun, Y.S., 2009. Cinnamon zeylanicum bark extract and powder mediated green synthesis of nano-crystalline silver particles and its bactericidal activity. Colloids Surf. B 73, 332–338.
Sihem, A., Lehocine, B.M., Miniai, H.A., 2012. Batch adsorption of phenol from industrial waste water using cereal by-products as a new adsorbent. Energy Procedia 18, 1135–1144.
Srihari, V., Ashotosh Das, 2009. Adsorption of phenol from aqueous media by an agro waste (Hemidesmus indicus) based activated carbon. Appl. Ecol. Environ. Res. 7 (1), 13–23.
Tabana, L., Tichapondwa, S., Labuschagne, F., Chirwa, E., 2020. Adsorption of phenol from wastewater using calcined magnesium-zinc-aluminium layered double hydroxide clay. Sustainability 12, 4273.
Vanaja, M., Paulkumar, K., Baburaja, M., Rajeshkumar, S., Gnanajobitha, G., Malarkodi, C., Sivakavinesan, M., Annadurai, G., 2014. Degradation of methylene blue using biologically synthesized silver nanoparticles. Bioinorg. Chem. Appl. 2014, 1–8.
Volesky, B., 2003. Sorption and Biosorption. BV-Sorbex Inc., Quebec, Canada.
Weber, W.J., Morris, J.C., 1963. Kinetics of Adsorption on Carbon From Solution. In: Journal of the Sanitary Engineering Division. American Society of Civil Engineers, pp. 31–60.
Yasmin, S., Nouren, S., Bhatti, H., Iqbal, D., Iftikhar, S., Majeed, J., Mustafa, R., Nisar, N., Nisar, J., Nazir, A., Iqbal, M., Rizvi, H., 2020. Green synthesis, characterization and photocatalytic applications of silver nanoparticles using Diospyros lotus. Green Process. Synth. 9 (1), 87–96.